CHAPTER 4

GEOCHEMISTRY

4.1 Sample Preparation

The carefully selected sixty-five Thoeng basaltic samples (as previously mentioned in Chapter 3) were prepared for whole-rock chemical analysis by firstly splitting into conveniently-sized fragments and then crushing into small thin chips (approximately 0.5 cm across), using a Rocklabs hydraulic splitter/crusher. These crushed fragments were cautiously chosen to avoid vesicles, amygdale minerals, veinlets, megacrysts and weathered surfaces. The selected chips were blown by compressed air to remove dusty materials. Approximately 70 g aliquots of the clean selected chips were pulverized for a few minutes using a Rocklabs tungsten-carbide ring mill. All the preparation procedures were done at Department of Geological Sciences, Chiang Mai University.

4.2 Analytical Techniques

All the powdered samples were analyzed for 12 major and minor oxides, including SiO_2, TiO_2, Al_2O_3, Fe_2O_3, FeO, MnO, MgO, CaO, Na_2O, K_2O, P_2O_5 and loss on ignition. In addition, forty-nine of these powdered samples were analyzed for Ba, Rb, Sr, Y, Zr, V, Ni and Cr, and sixteen of them were analyzed for Ba, Rb, Sr and Ni. Four representatives of these samples were analyzed for Nb, Th, U and rare-earth elements (Ce, La, Nd, Sm, Eu, Tb, Yb and Lu).

Almost all the analyses for major and minor oxides (SiO_2, TiO_2, Al_2O_3, total iron as Fe_2O_3, MnO, MgO, CaO, Na_2O, K_2O and P_2O_5), and trace elements (Ba, Rb, Sr, Y, Zr, Ni, Cr and V) were carried out on fusion discs using the X-ray fluorescence technique (XRF) by the staff of Rock and Mineral Analysis Section, Department of Mineral Resources, Bangkok. Detection limits for trace element analyses are 10 ppm.

FeO and ignition loss were measured by the author at Department of Geological Sciences, Chiang Mai University. FeO determination was done by using volumetric and titration method, whereas loss on ignition was gravimetrically determined by heating approximately 0.5 g of powdered sample at 1,050 °C for 1 hour.

The analyses of Nb, and Th, U and rare-earth elements (herein REE) were performed using the X-ray fluorescence and neutron activation techniques, respectively, by the staff of Chemex Labs Ltd. The code for Nb analysis is 191 (detection limit 2 ppm), while that for Th, U and rare-earth elements is RE-10(NAA)

of which detection limits for Th, U, Ce, La, Nd, Sm, Eu, Tb, Yb and Lu are 0.5, 1, 2, 1, 5, 0.1, 0.5, 0.5, 0.5 and 0.1 ppm in respective manner.

4.3 Magmatic Affinities and Rock Types

The studied Thoeng basaltic rocks (Appendix C) vary compositionally from basic to intermediate, as evidenced by their low values for SiO_2 and Mg/(Mg+Total Fe as Fe^{2+}) (herein mg#) that are in ranges of 47.9-54.8 wt% (average 49.8±1.6 wt%) and 0.41-0.57 (average 0.51±0.04), respectively. These basic-intermediate rocks have variable Na_2O+K_2O contents (2.0-6.1 wt%, 3.6±0.18 on average) with an averaged K_2O/Na_2O ratios of 0.43±0.14. Their Ni and Cr contents vary from 41 to 175 ppm and from 38-282 ppm, respectively. They form a compositional field straddling the demarcation line separating alkalic field from subalkalic field on total alkalis-silica diagram (Fig. 27); almost all are close to the field boundary on the subalkalic side. The Nb/Y ratios (0.38-1.04) of representative samples also lie well within the limits of subalkalic and mildly alkalic rocks (Pearce and Cann, 1973; Floyd and Winchester, 1975; Winchester and Floyd, 1977; Pearce, 1982). This implies that they could possibly well be either subalkalic or mildly alkalic rocks. However, the possibility of calc-alkalic affinities is not in agreement with their SiO_2, total iron as FeO (herein FeO*) and FeO*/MgO values as almost all Thoeng basaltic rocks lie in the compositional fields for tholeiitic rocks on SiO_2 and FeO* against FeO*/MgO diagrams (Fig. 28). Consequently, the Thoeng basaltic rocks are best assigned to transitional tholeiitic series.

According to the discrimination diagram for different rock types of Le Bas *et al.* (1986), the transitional tholeiitic lavas are constituted largely by basalts in restricted sense with subordinate basaltic andesites and a few trachybasalts (Fig. 27). In terms of normative compositions (Appendix C), the lavas classified as basalt, basaltic andesite and trachyandesite are olivine tholeiite and quartz tholeiite, quartz tholeiite and mildly alkalic basalt with normative nepheline up to 2.1%, respectively.

4.4 Major and Minor Oxides

It is well established that any suite of magmatic rocks related by crystal fractionation and unmodified by extensive crustal contamination should define coherent linear trends on appropriate variation diagrams. In this account, the data for major and minor oxides are plotted against differentiation index, defined as the sum of the weight percentage of normative quartz + orthoclase + albite + nepheline + leucite + kalsilite (Thornton and Tuttle, 1960), as shown in Figure 29. It appears that the data points for the studied samples form coherent trends; many trends exhibit remarkable inflection at a value for differentiation index of about 30. The trends for SiO_2, Al_2O_3 and CaO seem to be constant throughout a differentiation-index range of 20-30. However, in the more evolved lavas, the trends for SiO_2 and Al_2O_3 increase but those

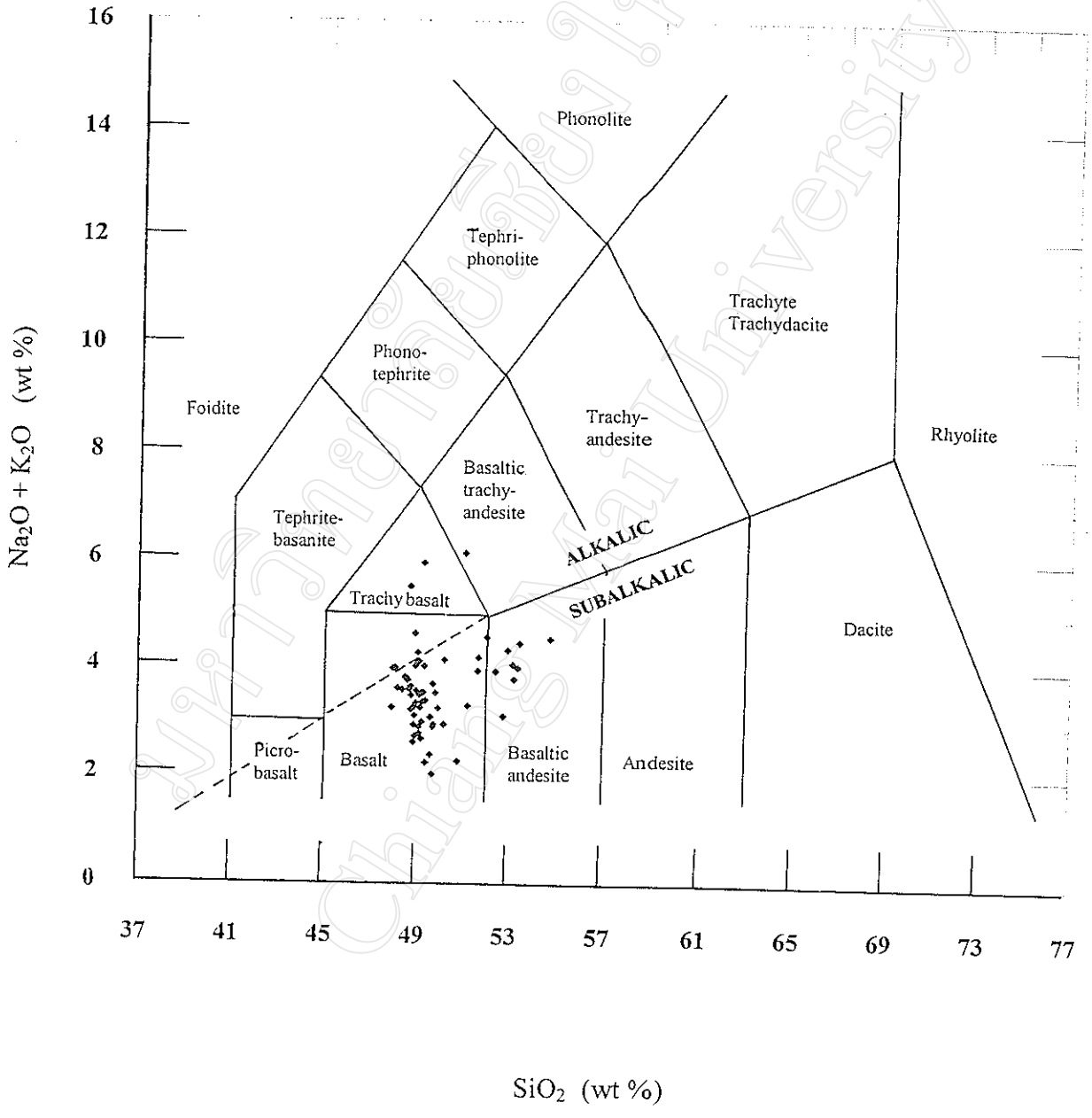

Figure 27 Alkali *versus* silica plot for analyzed Thoeng basaltic lavas. Delimited fields for different rock types are after Le Bas *et al.*,(1986). Also shown is alkalic/subalkalic dividing line of Miyashiro (1978).

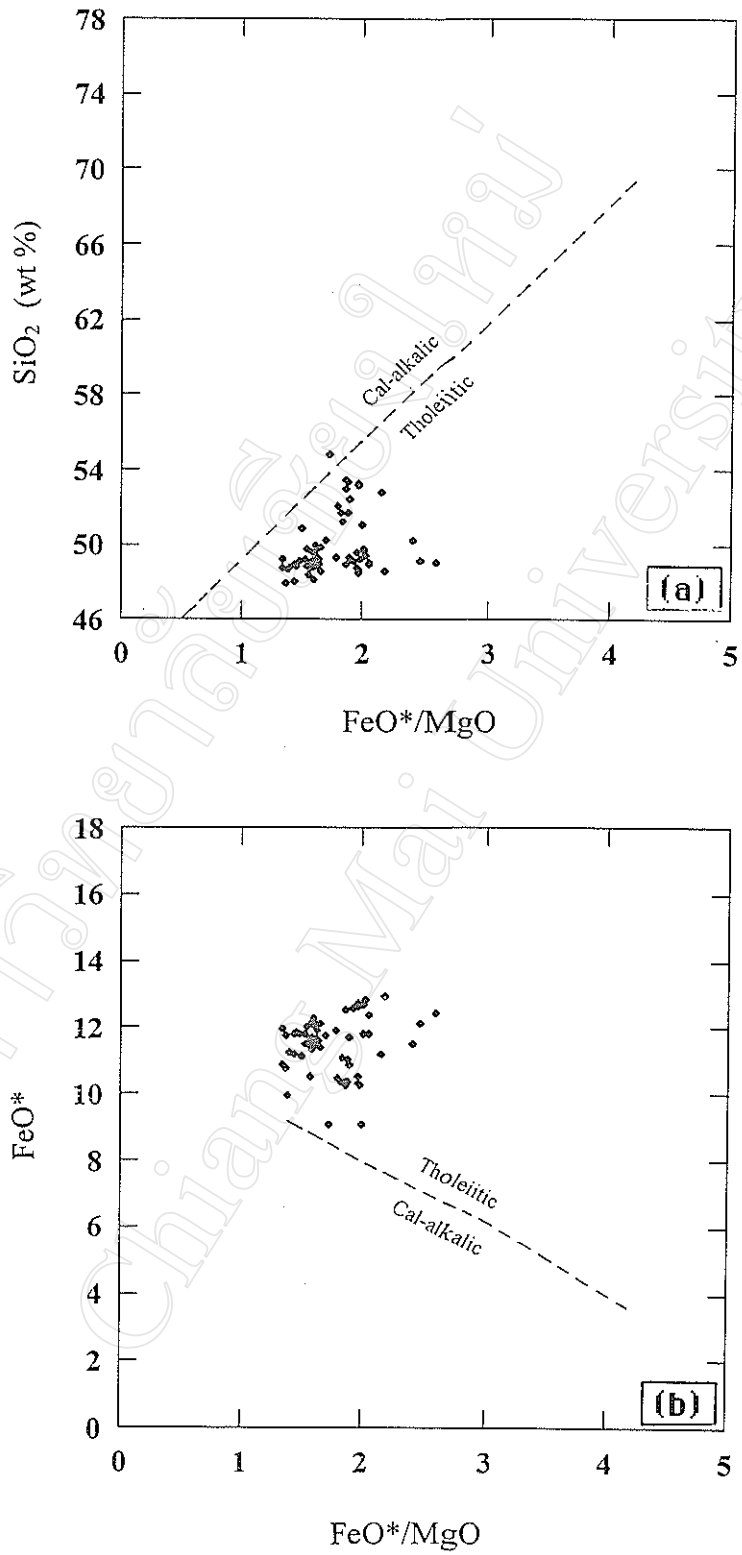

Figure 28 Plots of (a) SiO_2 and (b) FeO* against FeO*/MgO for basaltic rocks from Thoeng suite. Note that FeO* denotes total iron as FeO. Field boundaries between tholeiitic and calc-alkalic fields are taken from Miyashiro (1975).

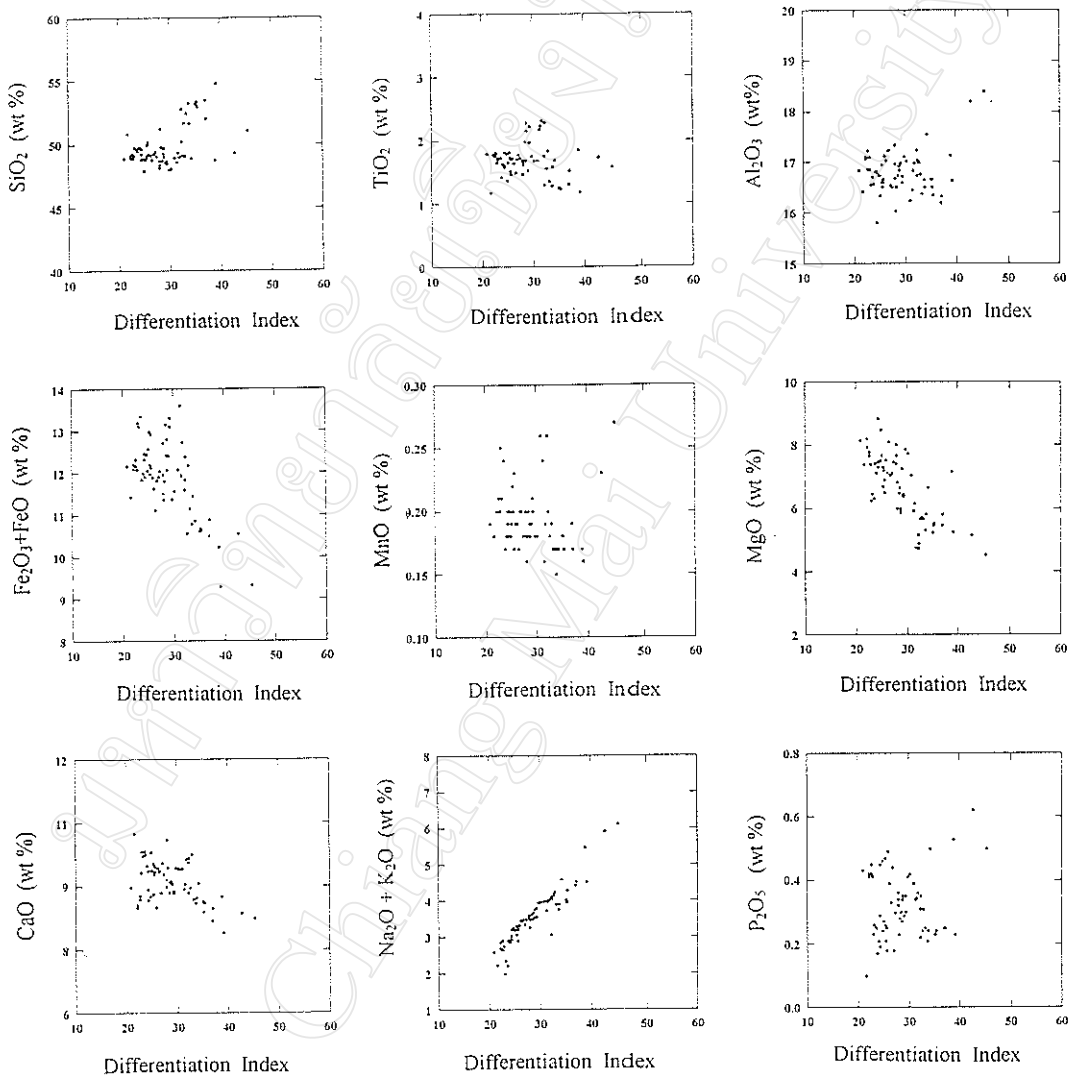

Figure 29 Major- and minor-oxide variation diagrams as a function of differentiation index for Thoeng transitional tholeiitic suite.

for CaO decrease with advancing fractionation. The trends for TiO_2 and $FeO+Fe_2O_3$ appear to ascend in the earlier stage and then descend in the later stage, typical of both tholeiitic and alkalic series. The trends for MgO and Na_2O+K_2O clearly form negative and positive patterns, respectively. The data points for P_2O_5 show a broad positive correlation with differentiation index, signifying that P_2O_5 is an incompatible element. In contrast to other oxides, MnO is quite scattered and does not define a trend.

The pattern of compositional trends is probably attributable to the different proportions of minerals separating from successive liquids. The line of descent might be controlled by removal of olivine, clinopyroxene and plagioclase in the earlier stage. Suppression of crystallization of Fe-Ti oxide phase might have included in the more differentiated liquids. The presence of olivine, plagioclase, clinopyroxene and Fe-Ti oxide phenocrysts and microphenocrysts (see Chapter 3) supports this deduction. Moreover, it is discernible from the variation diagrams that although the Thoeng basaltic suite clearly shows evidences for crustal contamination (see Chapter 3), the trends formed by the studied samples are governed significantly by crystal fractionation rather than crustal contamination.

4.5 Trace Elements

Using a similar fractionation parameter to major- and minor-oxide variation diagrams (Fig. 29), trace elements, including Ba, Rb, Sr, Zr, Y, Ni, Cr and V (Appendix D), in the Thoeng transitional tholeiitic suite also form broad compositional trends (Fig. 30). Ba, Rb, Sr, Zr and Y seem to increase, whereas Ni and Cr decrease with increasing differentiation. These suggest that Rb, Sr, Zr and Y are incompatible elements and that Ni and Cr are compatible elements. The incompatible nature of Sr, however, is not confirmed by plagioclase fractionation as previously mentioned. As a consequence, Sr is not considered to be an incompatible element. The depletion in Ni and Cr in the more evolved lavas record olivine fractionation. The enrichment of V in the early stage and the depletion of V in the later stage are in harmony with the patterns for TiO_2 and $FeO+Fe_2O_3$.

The relationships between incompatible-element pairs for Thoeng transitional tholeiitic suite, such as Ba-K, P-K, Y-Zr and Ba-Zr, are illustrated in Figures 31 and 32. They show linear trends with Ba/K = 0.01-0.04 (0.02±0.01 on average), P/K = 0.07-0.23 (0.17±0.04 on average), Zr/Y = 1.8-7.2 (4.0±1.1 on average) and Zr/Ba = 0.3-1.3 (0.6±0.2 on average), signifying that the basaltic rocks are comagmatic.

Up to present, many empirical diagrams for discriminating tectonic settings of eruption have been appeared in literatures (e.g. Pearce and Cann, 1973; Pearce and Norry, 1979; Pearce, 1980,1982; Shervais, 1982; Meschede, 1986). These diagrams are largely designed for basalts of tholeiitic affinities; a few can be applicable to transitional tholeiite and alkalic basalt. Therefore, the basalts of Thoeng suite are plotted only in terms of Ti-V (Fig. 33a), Ti/Y-Nb/Y (Fig. 33b), and Nb-Zr-Y (Fig. 34) to avoid ambiguous results. It appears that Thoeng basalts form a compositional field

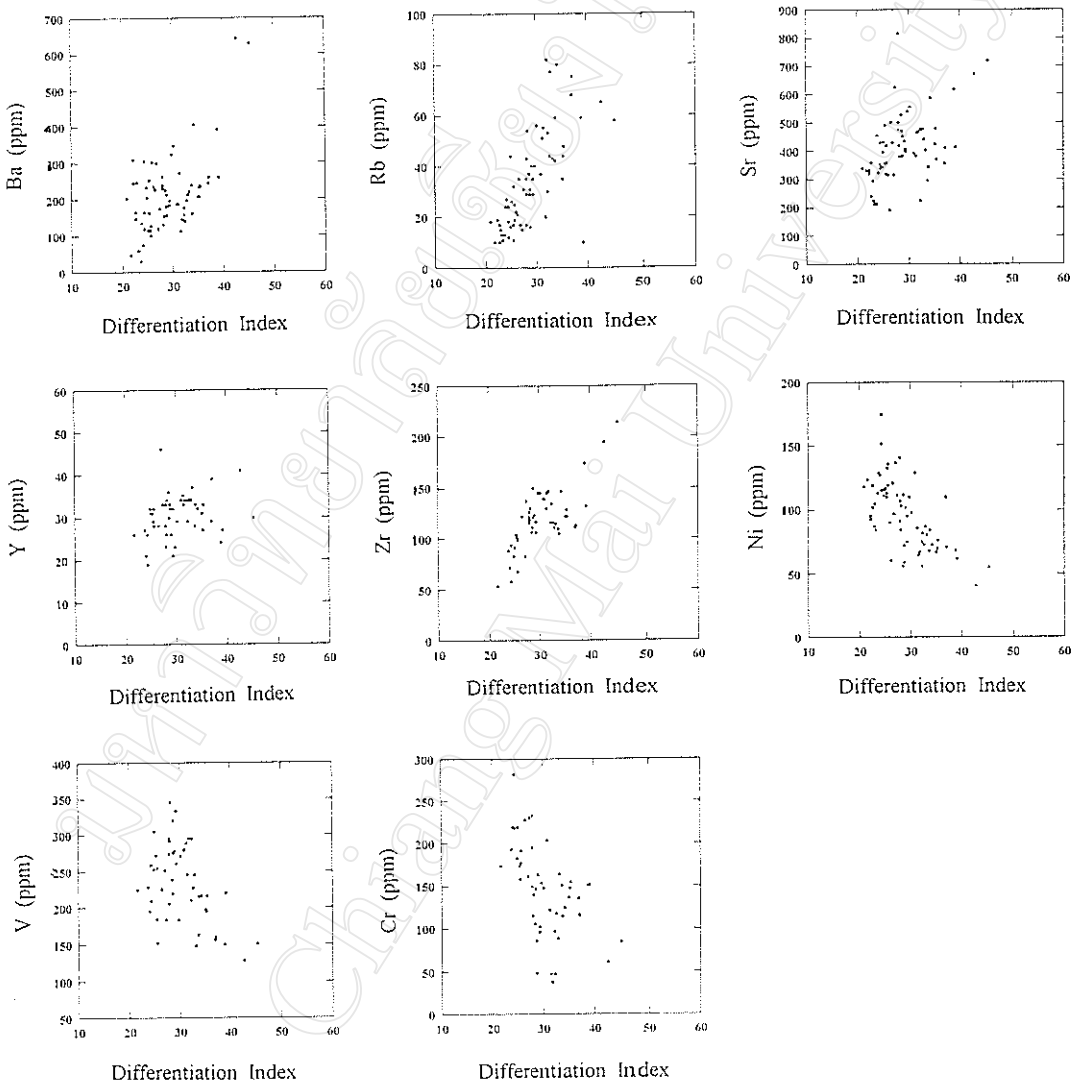

Figure 30 Distribution of trace elements as a function of differentiation index in Thoeng transitional basaltic rocks.

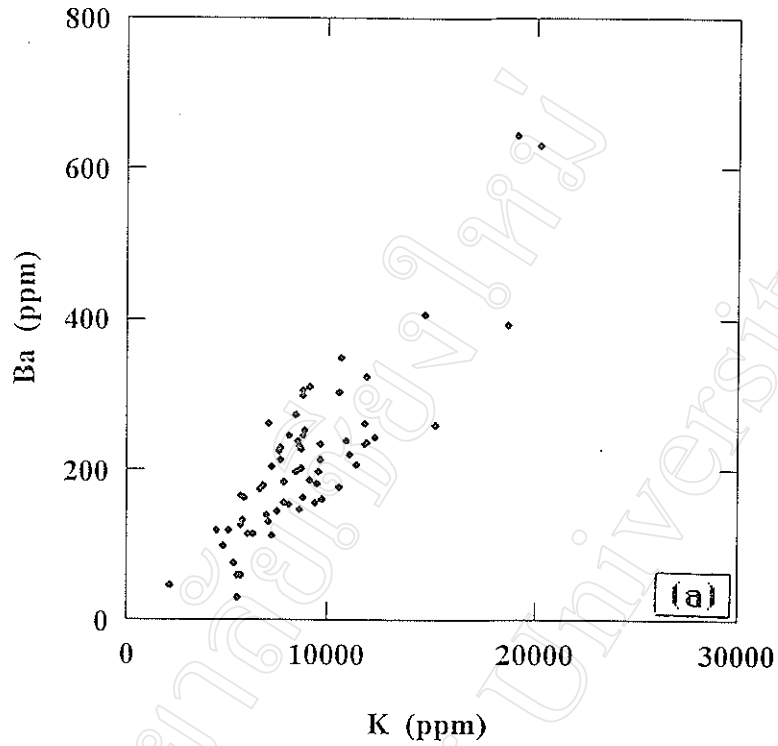

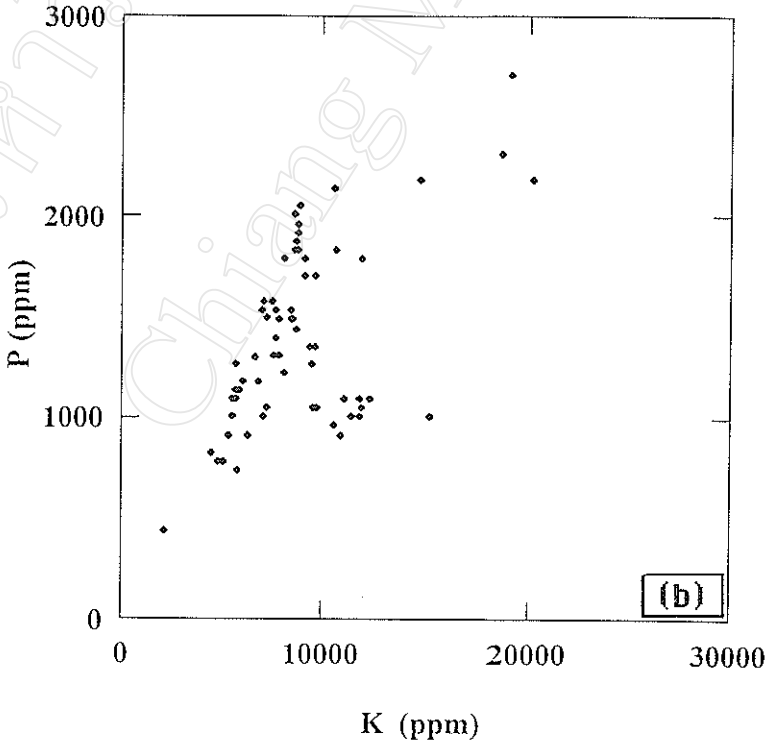

Figure 31 Variation of (a) Ba and (b) P with respect to K in basaltic rocks from Thoeng suite.

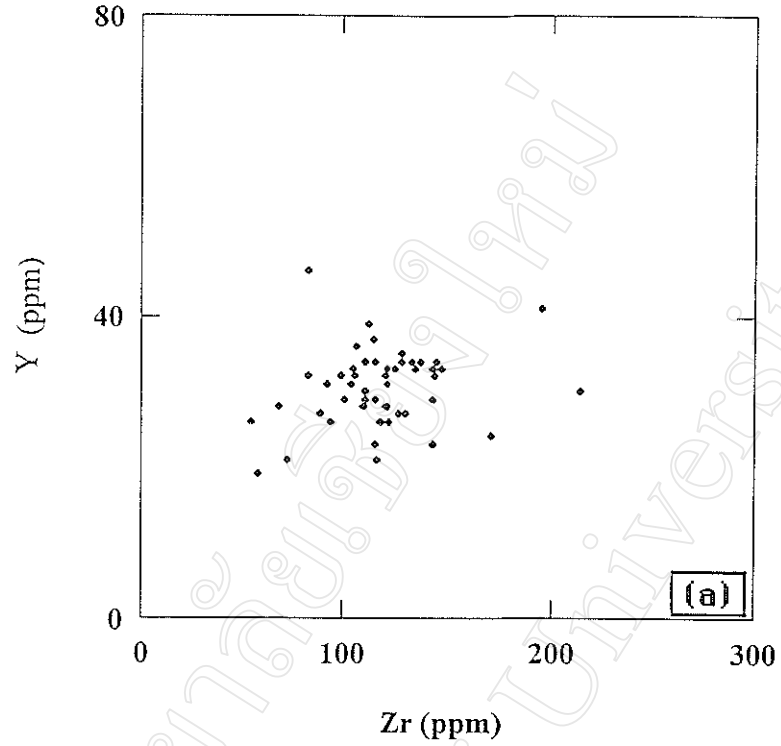

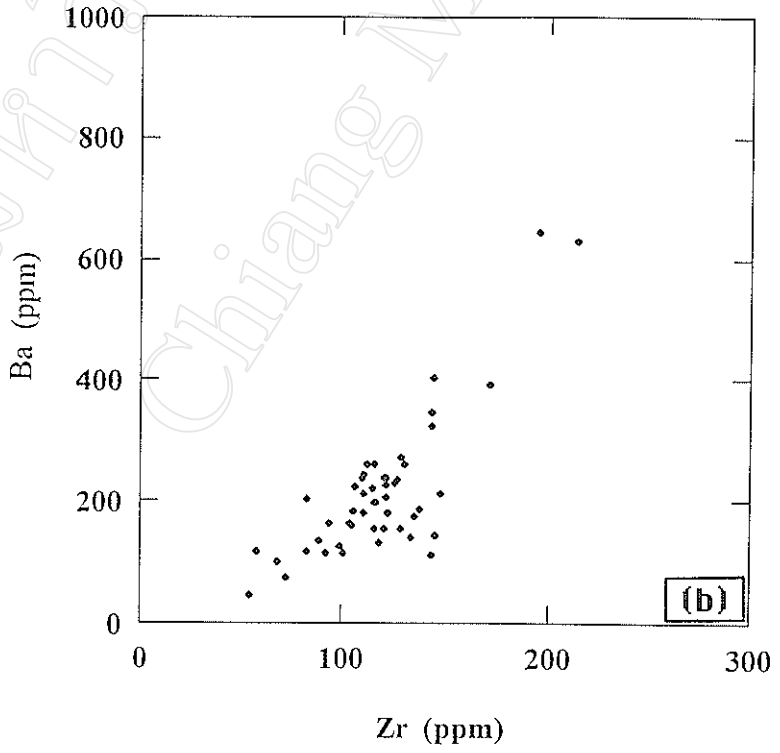

Figure 32 Correlation of (a) Y and Zr, and (b) Ba and Zr for all analyzed Thoeng transitional tholeiitic lavas.

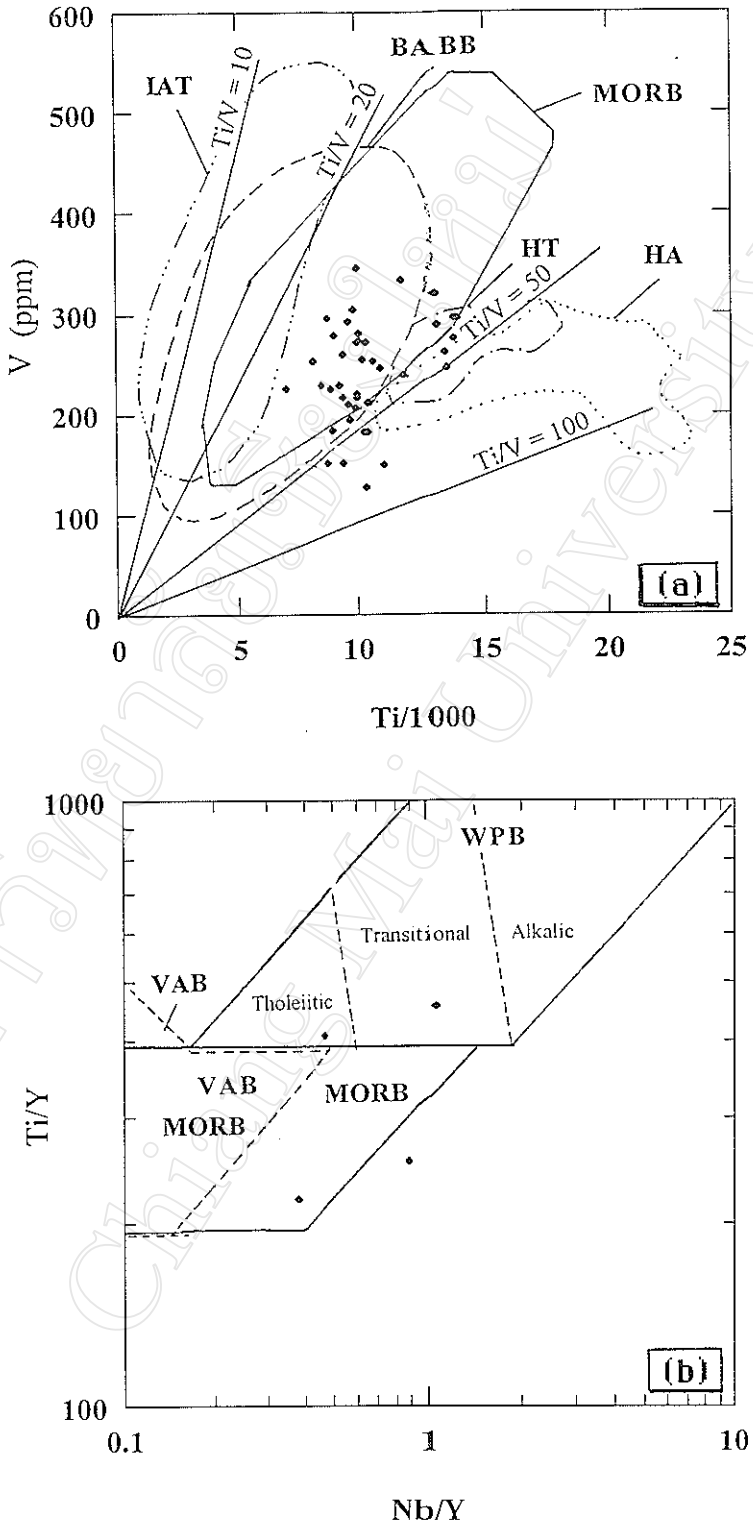

Figure 33 Tectonic discrimination diagrams in terms of (a) Ti and V (after Shervais, 1982), and (b) Ti/Y and Nb/Y(after Pearce, 1982) showing the distribution of analyzed Thoeng basalts. HA = Hawaiian alkalic basalt, HT = Hawaiian tholeiite, MORB = mid-ocean ridge basalt, BABB = back-arc basin basalt, IAT = island-arc tholeiite, WPB = within-plate basalt and VAB = volcanic arc basalt.

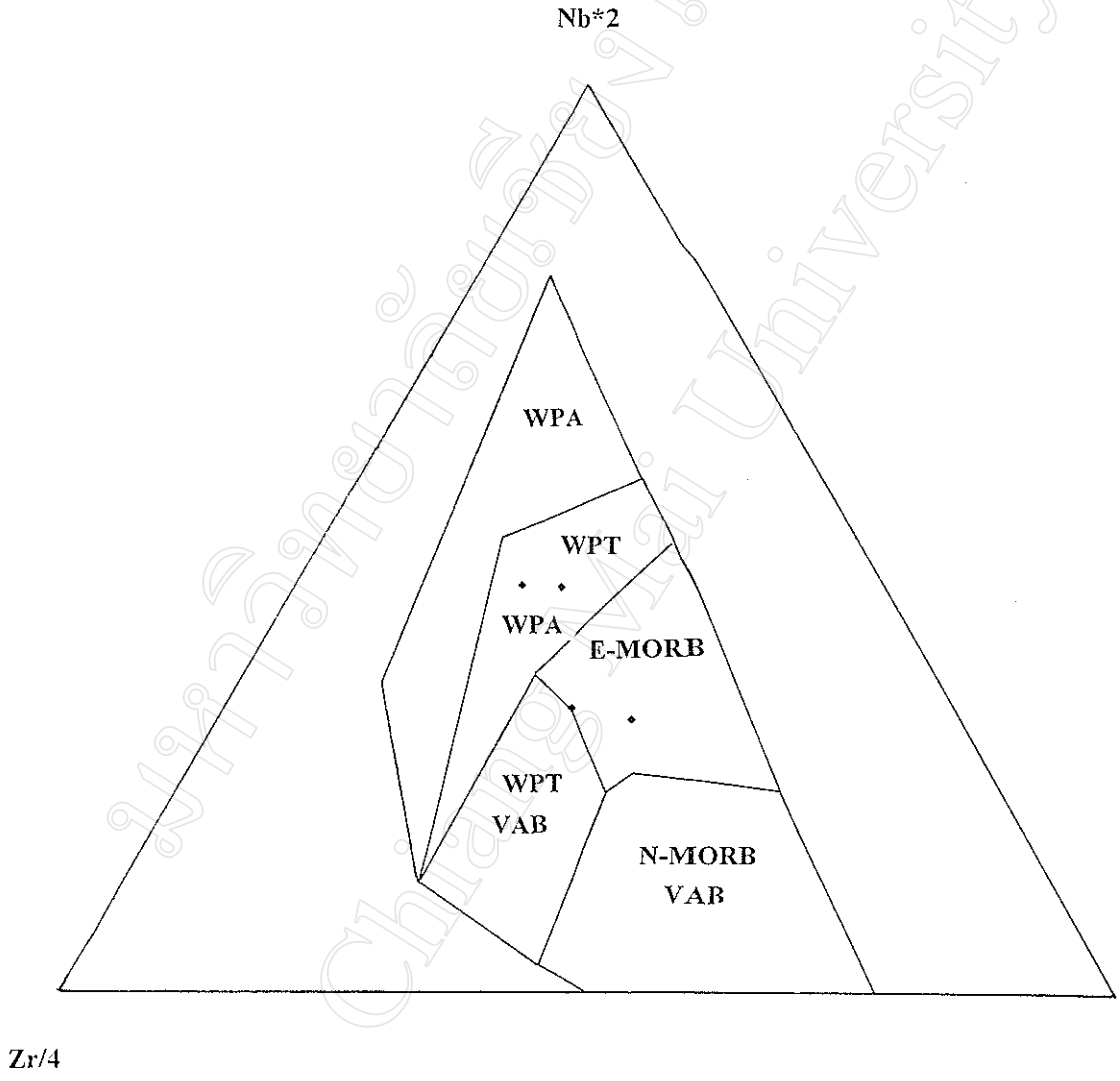

Figure 34 Nb-Zr-Y diagram for analyzed Thoeng basalt. Also shown are delimited fields for basalts of different tectonic environment (after Meschede, 1986). WPA = within-plate alkalic basalt, WPT = within-plate tholeiitic basalt, VAB = volcanic arc basalt, E-MORB = enriched mid-ocean ridge basalt and N-MORB = normal mid-ocean ridge basalt.

overlapping those of mid-ocean ridge basalts and within-plate (tholeiitic and alkalic) basalts. This appearance corresponds with their low values for Zr/Nb that range from 5.4 to 9.2 (Basaltic Volcanism Project, 1981).

4.6 Multi-element Patterns

REE analyses for four representatives of Thoeng basaltic suite are presented in Appendix D, and their chondrite-normalized values are plotted in Figure 35a. These samples have narrow ranges of chondrite-normalized values for REE, i.e. the values for La and Yb are in ranges of 41-82 and 10-12, respectively. The REE patterns show slight-moderate enrichment of light rare-earth elements (herein LREE) with chondrite-normalized La/Sm varying from 1.6 to 3.3 and are relatively depleted in heavy rare-earth elements (herein HREE) with chondrite-normalized Sm/Yb ranging from 1.5 to 2.5. These patterns are typical of within-plate tholeiites and transitional tholeiites, and obviously rule out the possible mid-ocean ridge affinities. The non-parallel and crosscut patterns may be arisen from analytical errors and/or variable degrees of crustal contamination as illustrated by petrographic evidences. Further isotopic studies are required to assess the hypothesis of crustal contamination.

So far, many sets of multi-element patterns have been proposed to characterize magmatic affinities. In this account, N-MORB normalized multi-element plot of Pearce (1982, 1983) has been applied to the representatives of Thoeng basaltic suite (Fig. 36a). The multi-element plot reveals step-like patterns analogous to the patterns for within-plate basalts and enriched mid-ocean ridge tholeiites.

Several recent studies, e.g. Holm (1982), Prestvik (1982), Duncan (1987) and Myers and Breitkopf (1989), have demonstrated that many empirical diagrams may often fail to clarify tectonic setting of eruption. Consequently, comparisons with modern lavas of different tectonic settings of formation have been carried out. The results, in terms of REE and N-MORB normalized multi-element patterns (Figs. 35 and 36), show that the Thoeng basaltic lavas are most analogous to the transitional tholeiitic lavas of Boina Centre in the Central Western Afar rift (Barberi *et al.*, 1975). It is important to mention here that the negative Sr anomalies in the highly differentiated rocks of Boina suite have resulted from alkali-feldspar fractionation. It can also be inferred on the basis of geochemical grounds that the Thoeng basaltic suite has been erupted in a continental rift environment. This interpretation is consistent with the tectonic history of Thailand that the eruption of the Late Cenozoic basalts took place after the continent-continent collision between Shan-Thai and Indochina for a long period of time (e.g. Bunopas and Vella, 1983; Barr and MacDonald, 1991; Intasopa, 1993).

4.7 Pearce Element Ratio Diagram

Pearce element ratios (Pearce, 1968) have been successfully applied by a number of workers (e.g. Nicholls, 1988; Russell and Nicholls, 1988; Stanley and

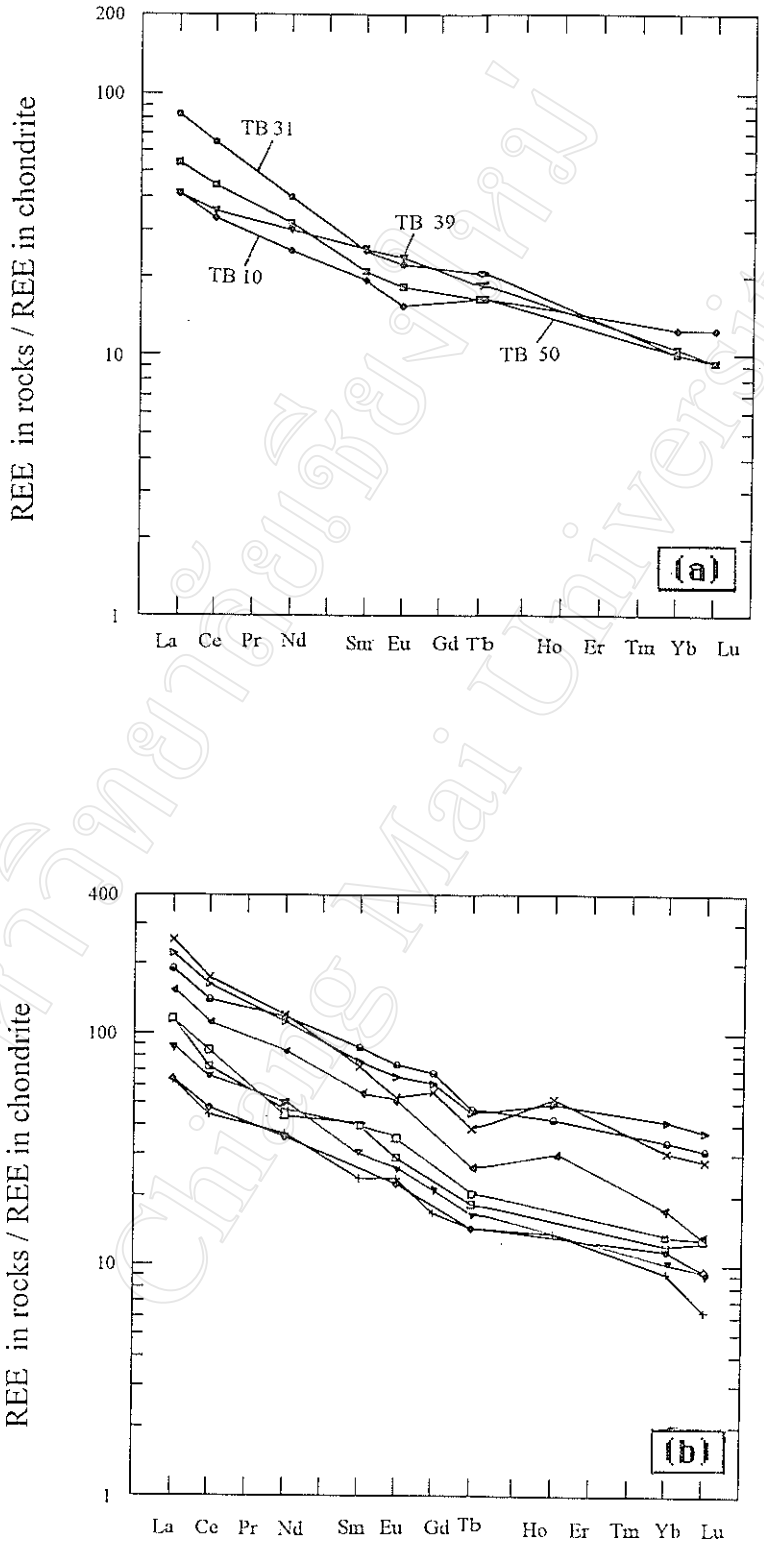

Figure 35 Chondrite-normalized REE data for Thoeng basaltic rocks (a) compared with those of Boina Centre, Central Western Afar rift (b). The data in (b) are taken from Barberi *et al.* (1975). Normalizing values used in both (a) and (b) are those of Taylor and Gorton (1977).

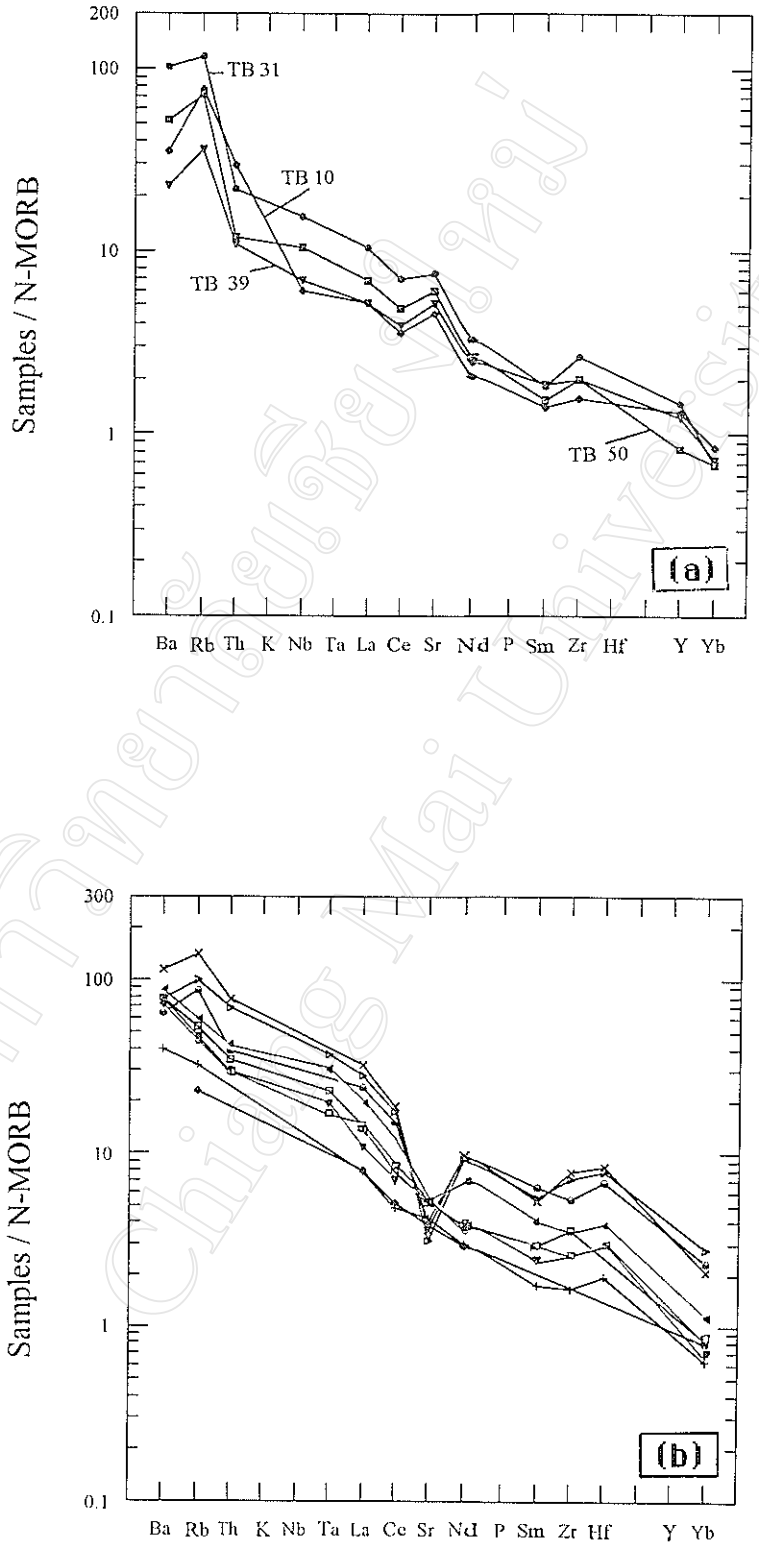

Figure 36 Multi-element diagram of Pearce (1982, 1983) displaying the patterns for Thoeng basaltic lavas (a) compared with those of Boina Centre, Central Western Afar rift (b). Source of data in (b) are the same as that in Figure 35. N-MORB normalizing values are those of Sun and McDonough (1989).

Russell, 1989; Trupia and Nicholls, 1996) to test whether the members of a rock suite are comagmatic, and estimate chemical changes caused by differentiation within one particular suite. Comagmatic rocks would have constant ratios of elements conserved in the system. In basaltic systems, some dispersed elements, such as K, P and Ti, are often conserved. The slope of trend presented on a Pearce element ratio diagram is sensitive to the stoichiometry of the crystallization and segregation phases. A judiceous choice of ratios as axes of the diagram provides a signature of the phases involved. A comagmatic origin of any rock suite can be recognized by Pearce element ratio diagram if a number of conserved elements are greater than 2. A plot of the ratios of two conserved elements over a common denominator (the third conserved element) would yield a tight cluster in case of comagmatic origin. Dispersion of element ratios implies that at least one of the applied elements is not conserved.

Pearce element ratios for Thoeng basaltic suite are listed in Appendix E. Useful parameters of Pearce element ratios in petrologic evaluation are also given in Table 2. Although Ti of the studied basaltic suite is not an incompatible element throughout the range of fractionation (see Sections 4.4 and 4.5), almost all the data points form a single fairly tight cluster on a Ti/K - P/K plot (Fig. 37). This signifies that the rocks are essentially comagmatic, as previously discussed, and Ti can be generally regarded as a conserved element. To assess the roles of olivine, plagioclase, clinopyroxene and Fe-Ti oxide involved in fractionation process, the studied samples are plotted in terms of some selected pairs of relevant parameters as listed in Table 2, i.e. olivine index (0.5(Mg+Fe)/n against Si/n) diagram (Fig. 38), plagioclase index ((2Na+Al)/n against Si/n) diagram (Fig. 39), olivine+plagioclase index (0.5(Mg+Fe) +2Ca+3Na)/n against Si/n) diagram (Fig. 40) and plagioclase/clinopyroxene index ((2 Ca+Na)/n against Al/n) diagram (Fig. 41). It is worth noting here that n represents a conserved element. These diagrams reveal that the basaltic rocks of Thoeng suite form linear patterns. The trends arisen from parameters using Ti as a normalizing value cannot be traced back to zero intercepts, whereas those using K and P as normalizing values have constant ratios for the related parameters. The nonzero intercepts might be caused by the fact that Ti is not a conserved element in the more evolved liquid. All the Pearce element ratio diagrams presented show that the trends of Thoeng basaltic rocks have slopes close to the stoichiometric line for plagioclase, implying that the liquid line of descent is mainly controlled by plagioclase separation. The patterns on olivine, plagioclase and olivine+plagioclase index diagrams also signify that olivine is an additional phase involved in fractionation process. The olivine index patterns preclude the fractionation of clinopyroxene and Fe-Ti oxide. It can be drawn at this stage that the overall chemical patterns of Thoeng basaltic rocks are almost totally resulted from abundant plagioclase and subordinate olivine fractionation. This is consistent with petrographic evidences that plagioclase and olivine are the most predominant phenocrysts/microphenocrysts.

Table 2 Summary of Pearce element ratios used in the evaluation of petrologic hypotheses. Element ratios are combined to test one (1), two (2), and three (3) phase segregation of Thoeng basalts. OL = olivine, PL = Plagioclase and CPX = Clinopyroxene (after Russell and Nicholls, 1988).

	Phase(s)	*X/n*	*Y/n*	Slope (M) expected	Other Phases
1	Olivine	0.5(Mg+Fe)	Si	OL = 1.0	CPX = 0.25; PL = 0.0
	Plagioclase	2Na + Al	Si	PL = 1.0	CPX = OL = 0.0
	Clinopyroxene	2Ca+Na-Al	Si	CPX = 1.0	PL = OL = 0.0
2	Olivine + Plagioclase	0.5(Mg+Fe)+2Ca+3Na	Si	OL+PL = 1.0	±CPX >1.0
	Plagioclase + Clinopyroxene	2Ca+ 3 Na	Si	PL + CPX = 1.0	±OL < 1.0
	Olivine + Clinopyroxene	0.5(Mg + Fe) + 1.5 Ca	Si	OL + CPX = 1.0	±PL < 1.0
3	Plagioclase Clinopyroxene	2Ca + Na	Al	CPX = α PL = 1.0	±OL = no effect

n = conserved constituent.
X and *Y* = elements plotted as x-axis and y-axis, respectively.

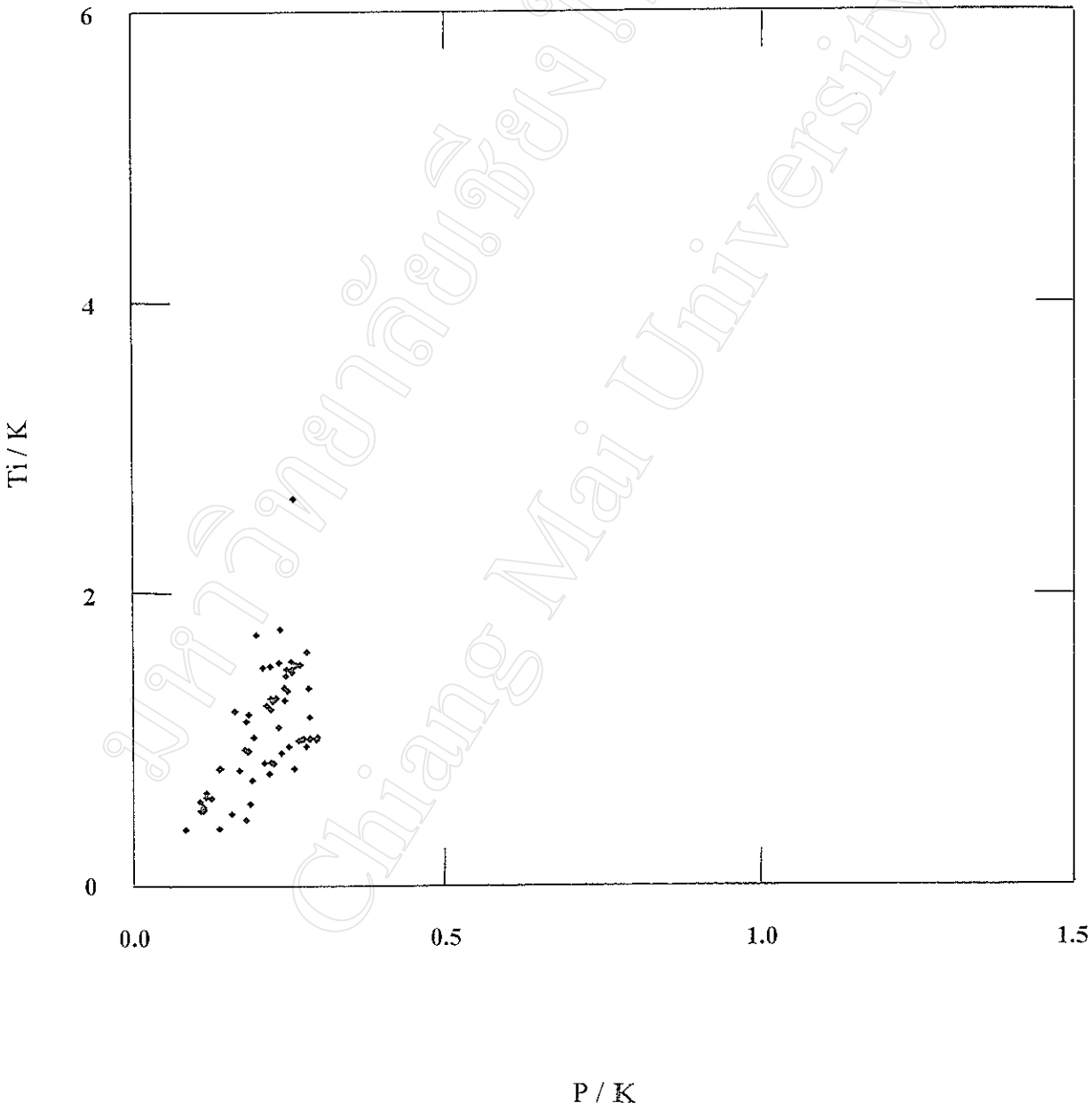

Figure 37 Correlation of Pearce element ratios Ti/K and P/K for analyzed Thoeng transitional tholeiitic lavas.

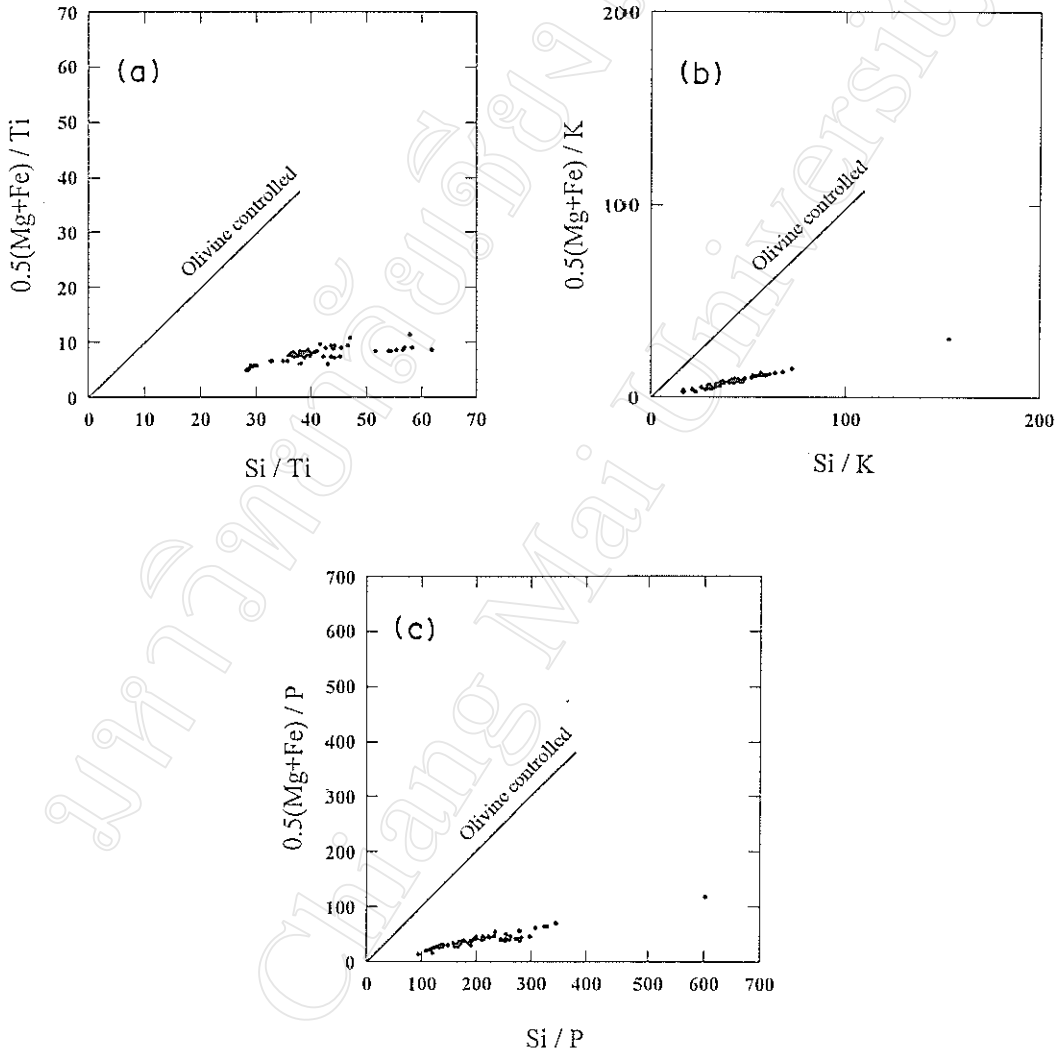

Figure 38 Olivine index diagram in terms of (a) 0.5(Mg+Fe)/Ti and Si/Ti, (b) 0.5(Mg+Fe)/K and Si/K and (c) 0.5(Mg+Fe)/P and Si/P for basaltic lavas of Thoeng transitional tholeiitic suite.

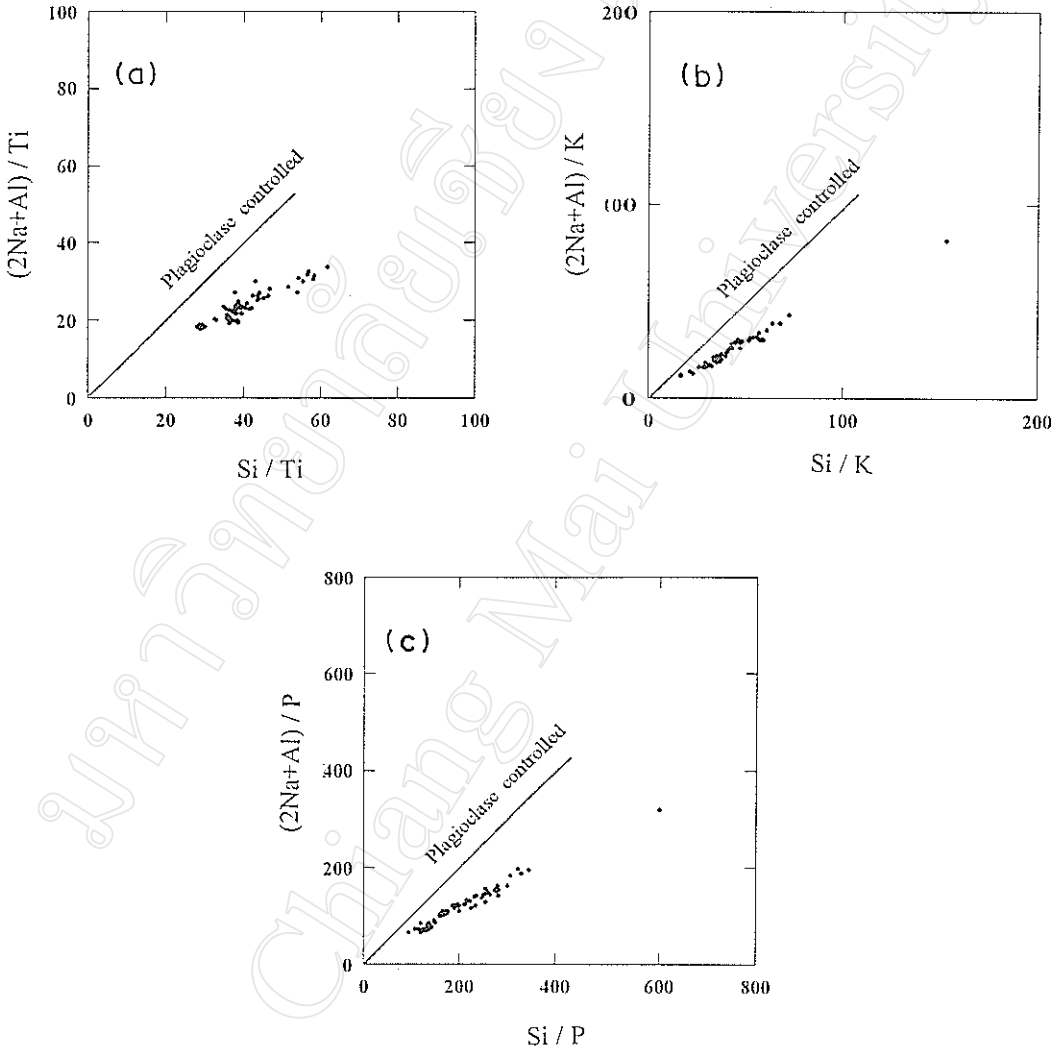

Figure 39 Plagioclase index diagram in terms of (a) (2Na+Al)/Ti and Si/Ti, (b) (2Na+Al)/K and Si/K and (c) (2Na+Al)/P and Si/P for basaltic lavas of Thoeng transitional tholeiitic suite.

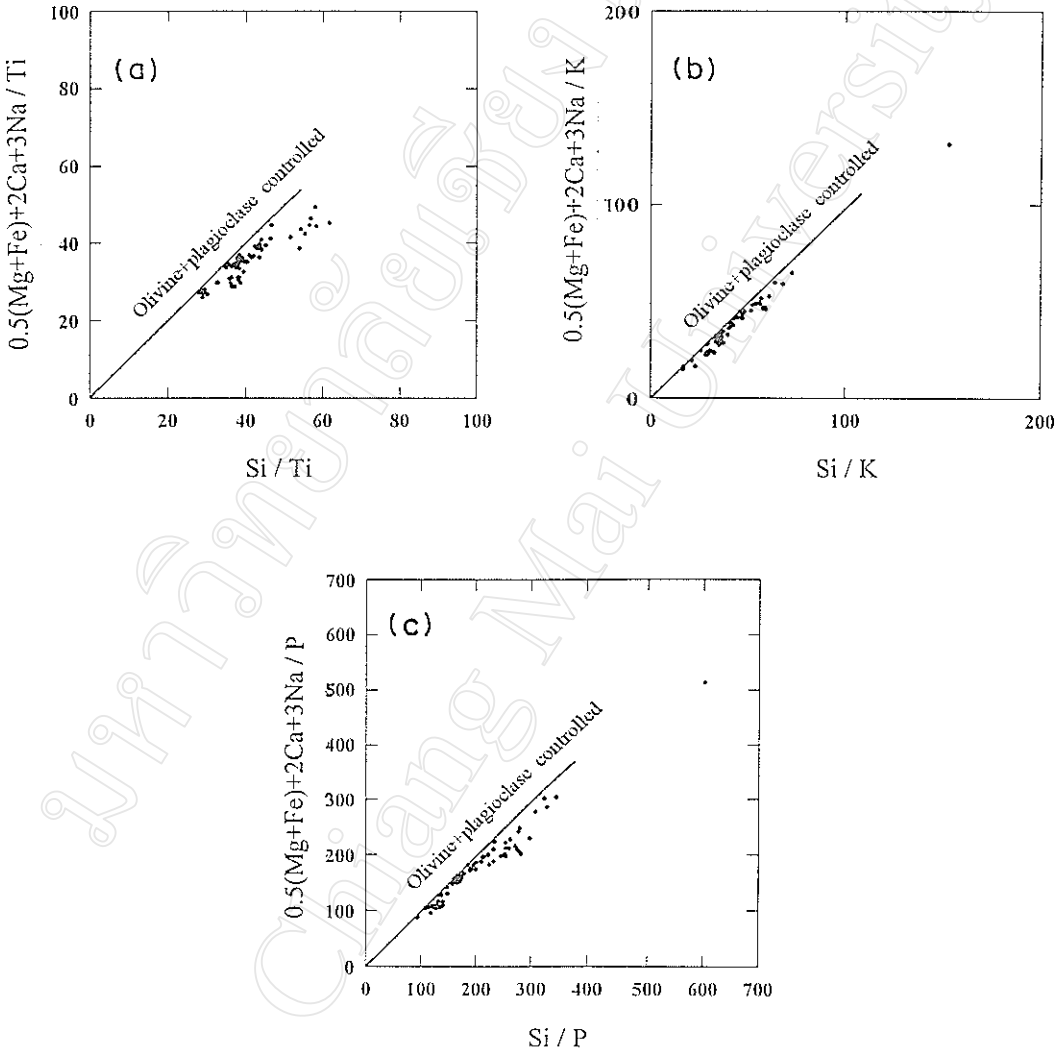

Figure 40 Olivine+plagioclase index diagram in terms of (a) (0.5(Mg+Fe)+2Ca+3Na) /Ti and Si/Ti, (b) (0.5(Mg+Fe)+2Ca+3Na)/K and Si/K and (c) (0.5(Mg+Fe)+ 2Ca+3Na)/P and Si/P for basaltic lavas of Thoeng transitional tholeiitic suite.

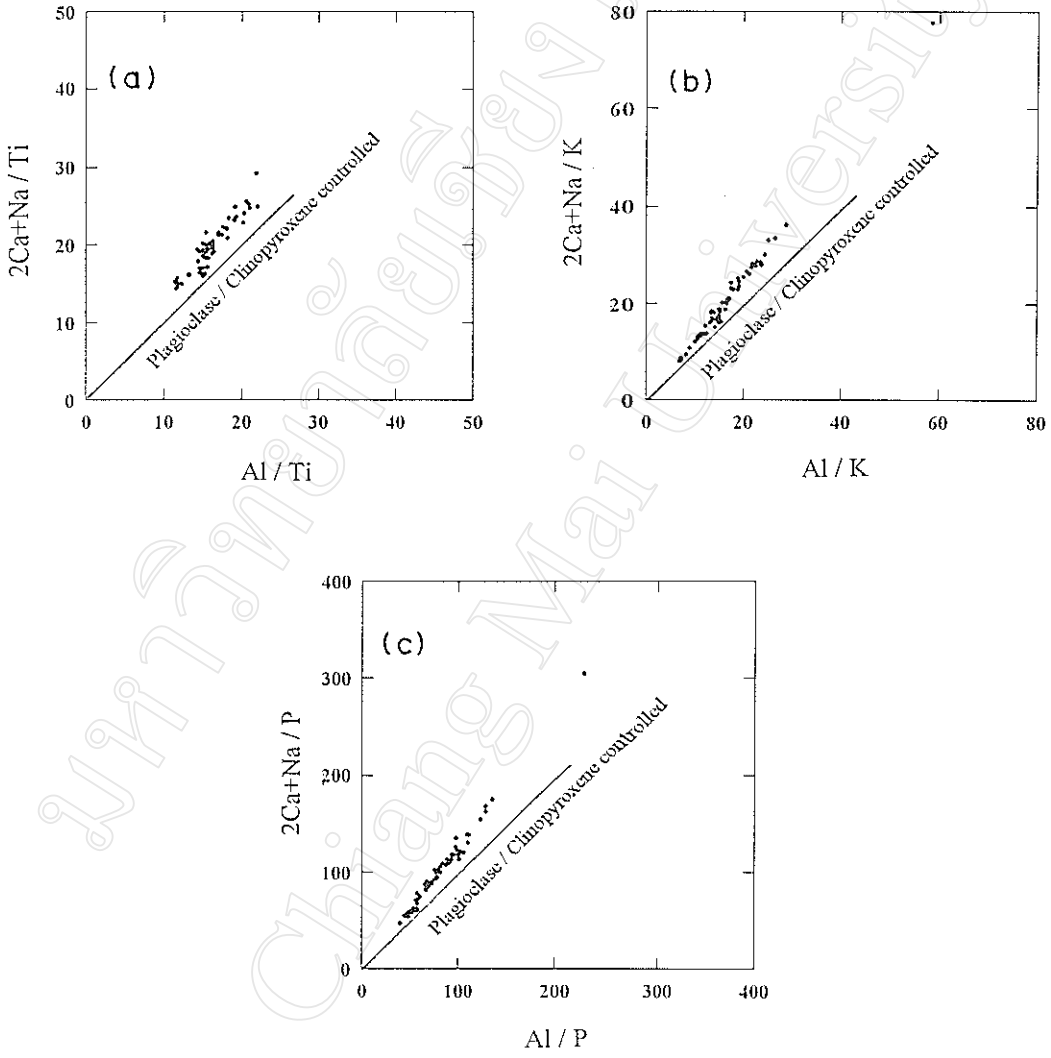

Figure 41 Plagioclase/clinopyroxene index diagram in terms of (a) (2Ca+Na)/Ti and Al/Ti, (b) (2Ca+Na)/K and Al/K and (c) (2Ca+Na)/P and Al/P for basaltic lavas of Thoeng transitional tholeiitic suite.